Available online at www.sciencedirect.com
SCIENCE DIRECT®
Applied Geochemistry 19 (2004) 379–393
Applied Geochemistry
www.elsevier.com/locate/apgeochem

Geological and anthropogenic factors influencing mercury speciation in mine wastes: an EXAFS spectroscopy study

Christopher S. Kim[a,*], James J. Rytuba[b], Gordon E. Brown Jr.[a,c]

[a]*Surface and Aqueous Geochemistry Group, Department of Geological and Environmental Sciences, Stanford University, Stanford, CA 94305-2115, USA*
[b]*US Geological Survey, 345 Middlefield Road, MS 901, Menlo Park, CA 94025, USA*
[c]*Stanford Synchrotron Radiation Laboratory, SLAC, 2575 Sand Hill Rd., MS 99, Menlo Park, CA 94025, USA*

Received 17 September 2002; accepted 17 June 2003
Editorial handling by W.B. Lyons

Abstract

The speciation of Hg is a critical determinant of its mobility, reactivity, and potential bioavailability in mine-impacted regions. Furthermore, Hg speciation in these complex natural systems is influenced by a number of physical, geological, and anthropogenic variables. In order to investigate the degree to which several of these variables may affect Hg speciation, extended X-ray absorption fine structure (EXAFS) spectroscopy was used to determine the Hg phases and relative proportions of these phases present in Hg-bearing wastes from selected mine-impacted regions in California and Nevada. The geological origin of Hg ore has a significant effect on Hg speciation in mine wastes. Specifically, samples collected from hot-spring Hg deposits were found to contain soluble Hg-chloride phases, while such phases were largely absent in samples from silica-carbonate Hg deposits; in both deposit types, however, Hg-sulfides in the form of cinnabar (HgS, hex.) and metacinnabar (HgS, cub.) dominate. Calcined wastes in which Hg ore was crushed and roasted in excess of 600 °C, contain high proportions of metacinnabar while the main Hg-containing phase in unroasted waste rock samples from the same mines is cinnabar. The calcining process is thought to promote the reconstructive phase transformation of cinnabar to metacinnabar, which typically occurs at 345 °C. The total Hg concentration in calcines is strongly correlated with particle size, with increases of nearly an order of magnitude in total Hg concentration between the 500–2000 μm and <45 μm size fractions (e.g., from 97–810 mg/kg Hg in calcines from the Sulphur Bank Mine, CA). The proportion of Hg-sulfides present also increased by 8–18% as particle size decreased over the same size range. This finding suggests that insoluble yet soft Hg-sulfides are subject to preferential mechanical weathering and become enriched in the fine-grained fraction, while soluble Hg phases are leached out more readily as particle size decreases. The speciation of Hg in mine wastes is similar to that in distributed sediments located downstream from the same waste piles, indicating that the transport of Hg from mine waste piles does not significantly impact Hg speciation. Hg L_{III}-EXAFS analysis of samples from Au mining regions, where elemental Hg(0) was introduced to aid in the Au recovery process, identified the presence of Hg-sulfides and schuetteite ($Hg_3O_2SO_4$), which may have formed as a result of long-term Hg(0) burial in reducing high-sulfide sediments.

1. Introduction

Elevated concentrations of Hg can be found in Hg mine- and Au mine-impacted regions, resulting in widespread contamination of the immediate mine site and

* Corresponding author at present address: Lawrence Berkeley National Laboratory, MS 70R0108B, 1 Cyclotron Road, Berkeley, CA 94720, USA. Fax: +1-510-486-7152.
E-mail address: cskim@lbl.gov (C.S. Kim).

0883-2927/$ - see front matter © 2003 Elsevier Ltd. All rights reserved.
doi:10.1016/S0883-2927(03)00147-1

surrounding environment. Mercury contamination is particularly prevalent in the California Coast Range, the source of the largest Hg mines in North America, where Hg mining occurred for over 100 a. The environmental impacts of Hg mining are still visible today in the large volumes of Hg-bearing waste rock and roasted ore (calcines) present at these mine sites, both containing high residual levels of Hg ranging in concentration from <100 to several 1000 mg/kg (ppm). Although Hg mining activity ended in the early 1970s, abandoned and untreated mine wastes continue to release Hg to nearby streams (Ganguli et al., 2000) and the atmosphere (Gustin et al., 2000; 2002a). Much of the Hg recovered from mining was transported to the Sierra Nevada region and used in Au recovery through an amalgamation and distillation process, resulting in the loss of approximately 3600 tons of elemental Hg (Churchill, 1999) which were distributed in nearby soils and sediments. Over time, weathering and surface water runoff have transported Hg-bearing wastes hundreds of km from their sources (Roth et al., 2001). The prevalence of Hg contamination throughout these areas poses a significant challenge to regulatory agencies attempting to limit the bioaccumulation of Hg in the food web, which leads to toxic levels of Hg in fish and poses a threat to human health.

The speciation of Hg in mine wastes is a critical factor in determining its mobility, reactivity, and potential bioavailability in mining regions. Since different Hg species possess varying degrees of solubility, the particular species present and their relative proportions in a Hg-contaminated region can greatly influence the release and transport of Hg from its source. Prior work using extended X-ray absorption fine structure (EXAFS) spectroscopy has demonstrated that Hg speciation can vary from mine to mine, although Hg-sulfides [cinnabar, HgS (hex.) and metacinnabar, HgS (cub.)] were found to be prevalent among calcines analyzed from five separate Hg mines in the California Coast Range (Kim et al., 2000). However, comparison of Hg speciation from mines with different geological histories indicated that speciation was influenced by the type of geological environment in which the Hg ore formed. Specifically, Hg-chloride minerals were identified in hot-spring Hg deposits where Cl concentrations are known to be elevated (Dickson and Tunell, 1968), while Hg deposits that formed in a silica-carbonate alteration rock lacked such Hg-chloride phases.

This prior study established EXAFS spectroscopy as a viable technique for directly determining the speciation of Hg in low-concentration ($\geqslant 100$ ppm Hg), heterogeneous, natural samples such as those from Hg-bearing mine wastes. These results also built upon previous EXAFS spectroscopy studies of the speciation of As (Foster et al., 1998), Pb (Cotter-Howells et al., 1994; Manceau et al., 1996; Morin et al., 1999; Ostergren et al., 1999), and Zn (O'Day et al., 1998; Manceau et al., 2000; Isaure et al., 2002; Juillot et al., 2003) in similar types of mining-impacted natural samples. Application of the EXAFS technique to determine Hg speciation in calibrated mixtures of model Hg compounds (Kim et al., 2000) and a comparison with results from EXAFS spectroscopy and sequential chemical extractions on the same samples (Kim et al., submitted for publications) further validated the use of EXAFS spectroscopy for determining Hg speciation in complex samples and better defined its limitations.

The speciation of Hg in natural environments is likely to be influenced by many factors in addition to the geology of the Hg deposit. These include particle size, distance from the point source, and processes such as ore roasting, weathering, or aging that can cause phase transformation of the primary HgS mineral or secondary Hg mineralization. The objective of this study is to determine the speciation of Hg in samples from a variety of mine-impacted environments using EXAFS spectroscopy and assess the degree to which the aforementioned variables affect Hg speciation. Determining the influence and importance of specific geological and anthropogenic variables on Hg speciation can provide insights about the processes of Hg release and distribution at these sites and the eventual fate of Hg in mine-impacted regions.

2. Experimental methods

The primary sampling region is indicated in Fig. 1 and encompasses many of the inactive Hg mine sites of the California Coast Range Hg mineral belt. Mercury-contaminated samples from former Au mine workings were also collected from the Carson River basin in western Nevada (not shown in figure). The sampled media included calcines, condenser soot, waste rock (unroasted Hg-bearing material deemed too low in concentration to classify as ore), distributed sediments, Hg-bearing Au mine tailings, and an amorphous Fe-oxyhydroxide precipitate forming downstream from an acid mine drainage seep at a Hg mine. Most samples contained Hg concentrations of 100 ppm or greater, although some samples with Hg concentrations below 100 ppm were also successfully analyzed using EXAFS spectroscopy. A summary of mine sites, media sampled, and total Hg concentrations is presented in Table 1.

Between 500 g and 1 kg of material was collected at each sampling site, with the top several cm of surficial material removed from the waste piles prior to collection in order to avoid sampling the most weathered material. All samples were stored in borosilicate glass jars with Teflon lids. Splits were sent to ChemEx Laboratories to determine total Hg concentration by aqua regia digestion and cold vapor atomic fluorescence spectrometry (CVAFS) according to US EPA Method

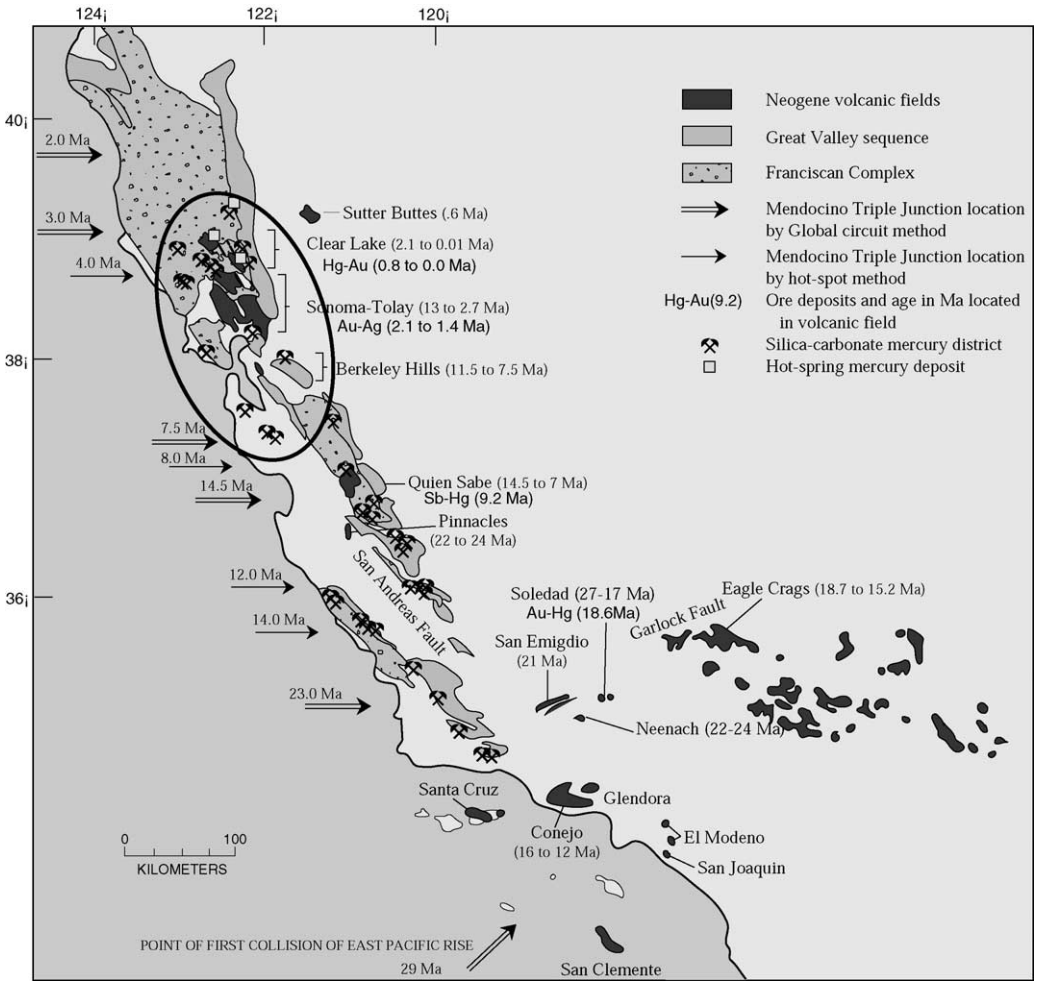

Fig. 1. Geologic map of Hg mining areas in the California Coast Range, distinguishing between silica-carbonate Hg deposits and hot-spring Hg deposits. Samples were primarily collected from a variety of mine waste media at multiple sites in the encircled region. From Rytuba (1996).

1631, which has estimated error limits of 5–10% (EPA, 2001). Wet samples (distributed sediments, Fe-precipitates) were refrigerated and dry samples maintained at room temperature prior to compositional analysis.

Bulk calcine and waste rock samples from several Hg mines were separated by particle size using a series of stainless steel sieves from W.S. Tyler, Inc. Two different sets of sieves, one from Stanford University and the other from the US Geological Survey (Menlo Park, CA office), were used to generate 9 or 11 separate splits, respectively, of each bulk sample. Table 2 lists the split number and size range of particles collected in each sieve for the two sets. The sieves were stacked and placed on a motorized shaker for 2 h to facilitate the physical separation of the bulk sample, at which point a split of each separated fraction was sent to ChemEx for total Hg analysis. Of the size fractions collected for the two sets of sieves, splits 3, 6 and 9 (corresponding to particle size ranges of 500–2000, 75–125, and <45 μm for the Stanford set and 1000–1700, 125–250, and 32–45 μm for the USGS set) were prepared for EXAFS analysis. Sieving was also conducted on samples from other mines with bulk Hg concentrations below 100 ppm, where the finest fraction (either <45 or <20 μm) was used for EXAFS analysis as a means of enriching the Hg content to a level sufficient for spectroscopic study.

EXAFS analysis was conducted on all samples using the protocol reported by Kim et al. (2000). Data were collected on wiggler-magnet beamlines 4–2, 4–3, and 11–2 at the Stanford Synchrotron Radiation Laboratory (SSRL) using Si(111) and Si(220) monochromator crystals. Hg L_{III}-edge EXAFS spectra were collected on the samples as dry powders at room temperature in the fluorescence-yield mode using a 13-element (beamlines 4–2 and 4–3) or 30-element (beamline 11–2), high-throughput Ge detector. This detection method is

Table 1
Summary of mine sites, sample IDs, media sampled, and total Hg concentrations

Mine location	Sample ID	Sampled media	Total Hg (ppm)
Aurora Mine, CA	20AU1C	Mine calcine (bulk)	700
Bessels Mill, NV	BMCR	Gold mill tailings	1070
Corona Mine, CA	CRC0997C4	Condenser soot	550
Dawson Mine, CA	21DS8	Downstream sediments	234
Dawson Mine, CA	21DUC10	Mine calcine (bulk)	78
Gambonini Mine, CA	GM-7	Mine calcine (bulk)	230
King Mine, CA	21K15C-S3	Mine calcine (split)	1386
King Mine, CA	21K15C-S6	Mine calcine (split)	2532
King Mine, CA	21K15C-S9	Mine calcine (split)	4115
Knoxville Mine, CA	21KN2C-S3	Mine calcine (split)	850
Knoxville Mine, CA	21KN2C-S6	Mine calcine (split)	2620
Knoxville Mine, CA	21KN2C-S9	Mine calcine (split)	5870
Knoxville Mine, CA	95KN4S	Fe-oxyhydroxide	220
Knoxville Mine, CA	MC-KN1B	Mine calcine (bulk)	277
McLaughlin Mine, CA	MC-MSP2	Mine calcine (bulk)	213
New Almaden Mine, CA	20NAC3	Condenser soot	19500
New Idria Mine, CA	20NI4C	Mine calcine (bulk)	310
New Idria Mine, CA	NISB	Mine calcine (split)	350
New Idria Mine, CA	NIS3	Mine calcine (split)	690
New Idria Mine, CA	NIS6	Mine calcine (split)	770
Oat Hill Mine, CA	OH0997C2	Mine calcine (bulk)	940
Ora Stimba Mine, CA	21OS-ORE	Waste rock (bulk)	1699
Ora Stimba Mine, CA	21ORS-1C	Mine calcine (bulk)	2104
Park & Bowie Mill, NV	PB1	Gold mill tailings	217
Reed Mine, CA	MC-RD2A	Waste rock (bulk)	188
San Carlos Mine, CA	SCT2	Mine tailings	500
Silver Cloud Mine, NV	UNRSC3 > 2	Mine calcine (bulk)	7240
Stulsaft Mine, CA	STWR3	Mine calcine (bulk)	200
Sulphur Bank, CA	SBS3	Mine calcine (split)	97
Sulphur Bank, CA	SBS6	Mine calcine (split)	440
Sulphur Bank, CA	SBS9	Mine calcine (split)	810
Sulphur Bank, CA	SBW9S3	Waste rock (split)	1580
Sulphur Bank, CA	SBW9S6	Waste rock (split)	22310
Sulphur Bank, CA	SBW9S9	Waste rock (split)	8120
Sulphur Bank, CA	SB01	Mine calcine (bulk)	250
Sulphur Bank, CA	TA1S3	Mine calcine (split)	230
Sulphur Bank, CA	TA1S6	Mine calcine (split)	200
Sulphur Bank, CA	TA1S9	Mine calcine (split)	300
Turkey Run Mine, CA	TR0997C2	Mine calcine (bulk)	1060

optimized for low-concentration samples (Waychunas and Brown, 1994). Six-absorption length As and Cr filters were used to attenuate elastic scattering, and Al filters served to minimize background matrix fluorescence.

The speciation of Hg in the unknown samples was determined by comparison of their EXAFS spectra with those from a Hg model compound spectral database. Previously collected EXAFS spectra of homogenous, well-characterized crystalline and sorbed Hg phases comprise the database, which is shown in Fig. 2. An EXAFS spectrum arises from the ejection of core-level photoelectrons from a central absorbing atom (Hg) which then scatter from first- and second-shells of neighboring atoms (Brown and Parks, 1989). The interference of the scattered photoelectron waves yields an EXAFS spectrum, which is sensitive to the arrangement and identity of atoms in the local vicinity of the absorber (up to $\sim$6 Å) and thus does not depend on long-range order. Assuming that the local environment of Hg in the various model compounds examined is sufficiently different, there will be corresponding differences among the EXAFS spectra of the different model compounds. Such differences are evident in the model spectra comprising the database (Fig. 2), and therefore the individual spectra can serve as unique fingerprints of component phases in a heterogeneous Hg-bearing sample.

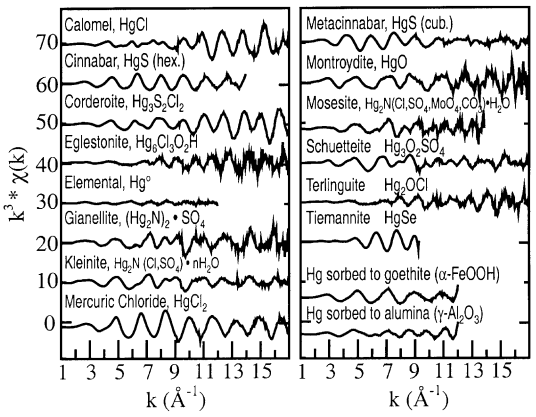

Fig. 2. EXAFS spectra of Hg minerals and Hg(II) sorption complexes in the model compound database used for linear least-squares fitting of the heterogeneous Hg-bearing samples. The horizontal axis represents the conversion of energy to momentum space following the normalization of the EXAFS data to a fixed point in energy space. The vertical axis is a *k*-cubed weighted expression of the EXAFS function, which is modeled as the sum of scattering contributions from each neighboring shell of atoms.

Table 2
Particle size ranges of mine waste size separations

Split #	Size range, Stanford (μm)	Size range, USGS (μm)
1	>2783	>2830
2	2000–2783	1700–2830
3	**500–2000**	**1000–1700**
4	250–500	500–1000
5	125–250	250–500
6	**75–125**	**125–250**
7	53–75	75–125
8	45–53	45–75
9	**<45**	**32–45**
10		20–32
11		**<20**

Two separate sets of sieves with slightly different size ranges were used. For both sets, splits 3, 6 and 9 (bold) were selected for EXAFS analysis to investigate the particle size dependency of Hg speciation. For samples with Hg concentrations <100 ppm, the finest size fraction (either <45 μm or <20 μm) was collected and prepared for EXAFS analysis.

While a model compound spectrum represents the spectral fingerprint of a single pure Hg phase, the EXAFS spectrum of a heterogeneous natural sample represents a composite of the EXAFS contributions from all Hg phases present, weighted according to the atom percent of Hg in the sample and influenced by the degree of structural order around Hg in each sample. In general, because EXAFS spectroscopy is sensitive only to the local structural environment around an absorbing atom, it can provide quantitative structural information about crystalline and even certain amorphous Hg-containing samples. However, when the radial disorder around Hg is sufficiently great [e.g. elemental Hg(0)], or if the first- and second-neighbor atoms in the local vicinity of Hg backscatter the ejected photoelectron too weakly (e.g., C atoms), the EXAFS spectrum will be damped in intensity. In either of these cases, the EXAFS spectrum may not be particularly useful in identifying such Hg phases, especially when in the presence of more structured crystalline Hg compounds. Assuming no such problems, the EXAFS spectrum collected from a natural sample containing multiple Hg phases can be decomposed using a linear least-squares fitting method into the sum of its individual components through direct comparison with the model compound spectra. Furthermore, determining the relative proportion of each model compound's contribution to the best possible linear combination fit allows quantification of the various phases present in a sample.

Using this protocol, the linear least-squares fitting program DATFIT, a component of the data analysis package EXAFSPAK (George and Pickering, 1995), was utilized to fit Hg L_{III}-EXAFS spectra of natural samples with the Hg L_{III}-EXAFS spectra in the model compound database over the *k*-range of 1–9 Å^{-1} for the lowest concentration samples or over the *k*-range of 1–12 Å^{-1} for the highest concentration samples. This difference in *k*-range is caused by the weak signal at higher *k*-values for low concentration samples, which makes EXAFS data collection at $k > 9$ Å^{-1} infeasible for low concentration samples. Single-component fits were first attempted in order to identify significant contributors (i.e., $\geqslant 10\%$ of the overall spectrum) to the final fit. This subset of significant components was then used to generate two-component fits and so on, repeating the process until no more significant contributors could be identified. The phases classified as contributing to the overall fit and the relative proportions in which they contribute, scaled to 100%, represent the final speciation of Hg in the sample. An example of such a linear fit of the Hg L_{III}-EXAFS spectrum of a Hg calcine sample from the Turkey Run Mine, CA is shown in Fig. 3. A residual value is assigned to each fit and represents the amount of the spectrum not accounted for by the linear combination procedure.

3. Results and discussion

3.1. Geological background

A comparison of Hg speciation as a function of Hg ore depositional environment is shown in Table 3. Previously published results (Kim et al., 2000) have been

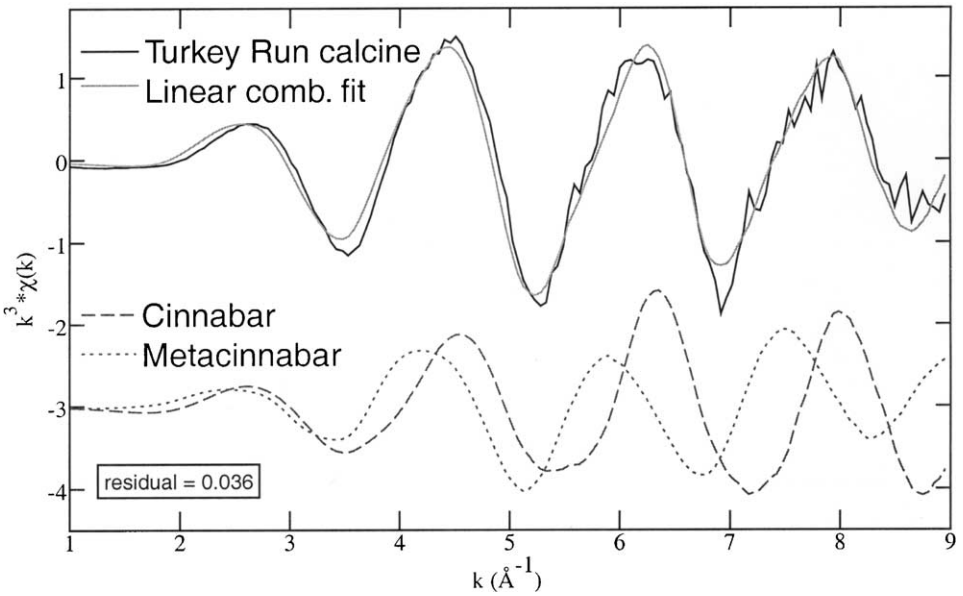

Fig. 3. Linear fitting results for the Turkey Run calcine, showing the natural EXAFS spectrum (black line), the linear combination fit (gray line), and the components which contribute to the linear fit (dashed lines). In this case, the calcine is found to consist of cinnabar and metacinnabar in proportions of 58 and 42%, respectively, when scaled to a total of 100%.

included in this table so that a wider geographical range of samples could be represented. Briefly, there are two primary types of Hg deposits in the California Coast Range, both associated with the impingement of the Mendocino Triple Junction (MTJ) off the coast of central California at 29 Ma, converting the region south of the MTJ from a subduction zone to a transform-fault system. This northwesterly-moving tectonic shift resulted in a slab window environment, allowing the hot aesthenosphere to upwell into the area formerly occupied by the subducting slab and inducing several episodes of magmatism and ore deposition which grow progressively younger moving from SE to NW (Fig. 1) (Rytuba, 1996).

The initial Hg ore deposits resulting from this thermal anomaly are termed silica-carbonate Hg deposits, in which Hg is deposited in the highly fractured zones of a brittle alteration rock consisting of silica and carbonate minerals. This silica-carbonate rock was initially formed by hydrothermal alteration of serpentinite bodies emplaced along fault zones such as the San Andreas Fault. The second type of Hg deposit is termed hot-spring Hg deposits, where Hg is deposited in low-temperature, near-surface active hydrothermal systems enriched in Cl^- and SO_4^{2-}. Occasional overprinting of both silica-carbonate and hot-spring Hg emplacement may occur, since the former is characterized by the initial high thermal flux of the slab window environment and the latter follows once this flux has subsided. Generally, however, the two types of deposits are fairly distinct from one another, as indicated in Fig. 1.

The majority of Hg in all samples is present as Hg-sulfides (Table 3), either as cinnabar or metacinnabar. Corderoite ($Hg_3S_2Cl_2$), a Hg-sulfide-chloride, was also observed in two samples from hot-spring Hg deposits. In addition, minor proportions of non-Hg-sulfide phases, such as mercuric chloride ($HgCl_2$), montroydite (HgO), schuetteite ($Hg_3O_2SO_4$), and terlinguite (Hg_2OCl), were identified in several of the samples. The high solubility of many of these phases compared to the extremely insoluble Hg-sulfides indicates that, although comprising a smaller percentage of the total Hg in the sample, these species may be disproportionately larger contributors of ionic Hg to the surrounding environment.

The influence of the Hg depositional environment on Hg speciation in mine wastes discussed earlier is also observed in the results of Table 3. Specifically, Hg-chloride phases are more common in samples collected at hot-spring Hg deposits, and are largely absent in samples collected at silica-carbonate Hg deposits. Some exceptions exist, such as the presence of mercuric chloride in samples from two silica-carbonate Hg mines (the San Carlos and Stulsaft mines), although this could be due to the aforementioned overprinting of a silica-carbonate Hg deposit with later hot-spring hydrothermal systems. Nevertheless, based on the range of samples analyzed, a general distinction in Hg speciation can be observed, with the presence of Hg-chloride phases as the primary difference between the two deposit types.

The prevalence of Hg-chloride phases in wastes from hot-spring Hg environments is thought to be linked to the local salinity levels in hot-spring depositional

Table 3
Hg speciation of mine wastes as a function of Hg ore depositional environment

Sample location (ID)	Locale	Material	Hg conc. (ppm)	EXAFS Speciation	Residual
Aurora Mine, CA (20AU1C)	Si-carbonate	Mine calcines	700	56% Metacinnabar, HgS (cub) 26% Montroydite, HgO 18% Cinnabar, HgS (hex)	0.045
Corona Mine, CA[a] (CRC0997C4)	Si-carbonate	Condenser soot	550	50% Cinnabar, HgS (hex) 39% Metacinnabar, HgS (cub) 11% Schuetteite, $Hg_3O_2SO_4$	0.052
Gambonini Mine, CA[a] (GM-7)	Si-carbonate	Mine calcines	230	58% Metacinnabar, HgS (cub) 42% Cinnabar, HgS (hex)	0.036
McLaughlin Mine, CA (MC-MSP2)	Si-carbonate	Mine calcines	213	48% Cinnabar, HgS (hex) 27% Montroydite, HgO 25% Metacinnabar, HgS (cub)	0.162
New Almaden Mine, CA (20NAC3)	Si-carbonate	Condenser soot	19500	75% Metacinnabar, HgS (cub) 25% Cinnabar, HgS (hex)	0.064
New Idria Mine, CA (20NI4C)	Si-carbonate	Mine calcines	310	61% Cinnabar, HgS (hex) 39% Metacinnabar, HgS (cub)	0.101
Reed Mine, CA (MC-RD2A)	Si-carbonate	Waste rock	188	61% Cinnabar, HgS (hex) 20% Metacinnabar, HgS (cub) 19% Schuetteite, $Hg_3O_2SO_4$	0.408
San Carlos Mine (SCT2)	Si-carbonate	Mine tailings	500	76% Cinnabar, HgS (hex) 24% Mercuric chloride, $HgCl_2$	0.427
Stulsaft Mine, CA (STWR3)	Si-carbonate	Mine calcines	200	48% Metacinnabar, HgS (cub) 39% Cinnabar, HgS (hex) 13% Mercuric chloride, $HgCl_2$	0.074
Turkey Run Mine, CA[a] (TR0997C2)	Si-carbonate	Mine calcines	1060	58% Metacinnabar, HgS (cub) 42% Cinnabar, HgS (hex)	0.036
Oat Hill Mine, CA[a] (OH0997C2)	Hot-spring	Mine calcines	940	58% Cinnabar, HgS (hex) 19% Mercuric chloride, $HgCl_2$ 13% Corderoite, $Hg_3S_2Cl_2$ 10% Terlinguite, Hg_2OCl	0.281
Silver Cloud Mine, NV (UNRSC3 > 2)	Hot-spring	Mine calcines	7240	84% Cinnabar, HgS (hex) 16% Mercuric chloride, $HgCl_2$	0.270
Sulphur Bank, CA[a] (SB01)	Hot-spring	Mine calcines	250	46% Metacinnabar, HgS (cub) 34% Corderoite, $Hg_3S_2Cl_2$ 20% Cinnabar, HgS (hex)	0.186

[a] Data from previous study (Kim et al., 2000).

systems relative to those of silica-carbonate deposits. During the deposition and mining of Hg in hot-spring environments, Hg-chloride phases may form during (1) initial Hg ore deposition, (2) the roasting process, and/or (3) later chemical weathering reactions. The low to moderate salinity levels in these regions, which average between 0.5 and 2.5 wt.% NaCl based on fluid inclusion studies (Henley, 1985; Sherlock et al., 1995), may be sufficient to produce minor amounts of Hg-chloride phases, particularly if hydrothermal boiling generates localized areas of elevated salinity and subsequent supersaturation of Hg-chlorides (Drummond and Ohmoto, 1985). In comparison, studies of hydrothermal fluids associated with silica-carbonate Hg deposits show that silica and CO_2 are the dominant components in solution (Barnes et al., 1973a,b; Peabody and Einaudi, 1992; Sherlock and Logan, 1995), implying that associated chloride levels were low. These differences aside, the possibility of Hg-chloride formation during initial ore deposition in hot-spring environments is unlikely due to the relatively low salinity levels, the infrequency of high-salinity regions due to boiling (Sherlock et al., 1995), and the lack of identifiable Hg-chlorides in these deposits based on both field studies and EXAFS analyses (see the analyses of Sulphur Bank waste rock samples in Tables 4 and 5).

The high-temperature roasting of Hg ores and subsequent cooling of the volatilized phases in a series of columns designed to condense elemental Hg(0) for collection is a more likely process by which Hg-chloride phases may form. Due to the inefficiency of the Hg calcining procedure, residual Hg present in the calcines (ranging in concentration from the 100s to 1000s of ppm Hg) could have reacted with available Cl^- to form Hg-chloride phases during roasting. Chloride could become available during roasting by the vaporization of

Table 4
Hg speciation of calcine and waste rock samples from the same mine to compare potential effects of ore roasting on speciation

Sample location (ID)	Materials	Hg conc. (ppm)	EXAFS Speciation	Residual
Ora Stimba Mine, CA				
(21OS-ORE)	Waste rock	1699	81% Cinnabar, HgS (hex) 19% Metacinnabar, HgS (cub)	0.042
(21ORS-1C)	Mine calcines	2104	89% Metacinnabar, HgS (cub) 11% Cinnabar, HgS (hex)	0.039
Sulphur Bank, CA				
(SBW9S6)	Waste rock	22310	100% Cinnabar, HgS (hex)	0.107
(SB01)	Mine calcines	250	46% Metacinnabar, HgS (cub) 34% Corderoite, $Hg_3S_2Cl_2$ 20% Cinnabar, HgS (hex)	0.186

remnant water or the decomposition of the abundant hydrothermal alteration products, particularly clays (White and Roberson, 1962; Dickson and Tunell, 1968), which had been bathed in saline fluids and likely retained elevated concentrations of Cl^-. Upon disposal of the calcines in large tailings piles, exposure to weathering processes and repeated wetting and drying cycles may also have induced dissolution and reprecipitation of soluble Hg-chlorides over time. Although it is not possible to conclusively determine the process(es) of formation for the Hg-chlorides detected by EXAFS spectroscopy, the general distinction in Hg speciation between the two types of deposits is compatible with the different geochemical environments of these systems.

3.2. Roasting process

As previously mentioned, Hg-sulfides in the form of cinnabar and metacinnabar constitute the highest proportion of Hg-containing phases in all of the samples analyzed, consistent with the fact that cinnabar is the primary ore mineral in Hg deposits. However, the proportions of metacinnabar detected in several calcine samples (Table 3), where up to 75% metacinnabar was identified, are much higher than anticipated based on field studies of Hg ore deposits, which only rarely report minor proportions of metacinnabar. Although the presence of metacinnabar may have been overlooked in field studies due to its black color compared to the deep red hue of cinnabar, the transformation of cinnabar to metacinnabar during the roasting process is a likely explanation for the elevated metacinnabar levels detected in these calcines.

Table 4 shows Hg speciation results for Hg-bearing mine wastes from the Sulphur Bank and Ora Stimba mines. At both mines, a calcine pile and waste rock pile were sampled to assess potential effects of ore roasting on Hg speciation. The results show that cinnabar is the dominant Hg phase in the unroasted waste rock samples (present in proportions from 81 to 100%), while metacinnabar is more prevalent in the calcines (46–81%). This suggests that ore roasting converts cinnabar to metacinnabar by heating it above the cinnabar-metacinnabar inversion temperature of 345 °C (Kullerud, 1965). Mercury ore was crushed and then roasted in excess of 600 °C to release Hg as volatile elemental Hg(0) gas (Rytuba, 2000), thereby providing temperatures sufficient to cause the conversion of non-released cinnabar to metacinnabar. Such a process may also have introduced impurities such as Fe, Se, and Zn that impeded the conversion back to cinnabar upon cooling and are more common to the metacinnabar structure (Dickson and Tunell, 1959; Tauson and Akimov, 1997). This origin of metacinnabar is consistent with the noted high levels of metacinnabar in the calcines analyzed (Table 3) and supports the proposed formation of metacinnabar through ore roasting.

The presence of corderoite in the Sulphur Bank calcine sample implies that this phase may also have formed through secondary processes, either as a result of ore roasting or the prolonged weathering of the exposed material. The generation of volatile $HgCl_2$ and H_2S gases during roasting, for example, would provide the reactants necessary for corderoite formation as demonstrated experimentally (Carlson, 1967). Additionally, the high Cl^- and low pH environment of the Sulphur Bank mine is conducive to corderoite formation (Foord and Berendsen, 1974; Parks and Nordstrom, 1979; Paquette and Helz, 1995), indicating that it could also be a primary Hg mineral in the initial hot-spring ore deposit.

3.3. Particle size

Mercury speciation results of selected sieved fractions from mine calcine and waste rock samples are shown in Table 5. As particle size decreases within each bulk sample the total Hg concentration generally increases, in some cases by nearly an order of magnitude (e.g., a

Table 5
Hg speciation of selected sieved fractions of Hg mine waste samples, including particle size range from sieving, total Hg concentration, and proportion of Hg-sulfides

Mine	Size range (μm)	Hg conc. (ppm)	EXAFS Speciation	Σ Hg-sulfides (%)	Residual
King					
(21K15C-S3)	1000–1700	1386	49% Metacinnabar, HgS (cub) 34% Cinnabar, HgS (hex) 17% Montroydite, HgO	83	0.103
(21K15C-S6)	125–250	2532	58% Metacinnabar, HgS (cub) 24% Cinnabar, HgS (hex) 18% Tiemannite, HgSe	82	0.091
(21K15C-S9)	32–45	4115	59% Metacinnabar, HgS (cub) 41% Cinnabar, HgS (hex)	100	0.059
Knoxville					
(21KN2C-S3)	1000–1700	850	43% Cinnabar, HgS (hex) 33% Metacinnabar, HgS (cub) 24% Montroydite, HgO	76	0.075
(21KN2C-S6)	125–250	2620	48% Cinnabar, HgS (hex) 27% Metacinnabar, HgS (cub) 25% Montroydite, HgO	75	0.051
(21KN2C-S9)	32–45	5870	55% Cinnabar, HgS (hex) 28% Metacinnabar, HgS (cub) 17% Montroydite, HgO	83	0.044
New Idria					
(NISB)	500–2000	350	56% Cinnabar, HgS (hex) 22% Montroydite, HgO 22% Eglestonite, $Hg_3Cl_3O_2H$	56	0.138
(NIS3)	75–125	690	59% Cinnabar, HgS (hex) 31% Montroydite, HgO 10% Metacinnabar, HgS (cub)	69	0.061
(NIS6)	<45	770	48% Cinnabar, HgS (hex) 21% Corderoite, $Hg_3S_3Cl_2$ 16% Eglestonite, $Hg_3Cl_3O_2H$ 15% Montroydite, HgO	69	0.086
Sulphur Bank					
(SBS3)	500–2000	97	89% Metacinnabar, HgS (cub) 11% Mercuric chloride, $HgCl_2$	89	0.091
(SBS6)	75–125	440	82% Metacinnabar, HgS (cub) 18% Cinnabar, HgS (hex)	100	0.043
(SBS9)	<45	810	85% Metacinnabar, HgS (cub) 15% Cinnabar, HgS (hex)	100	0.029
Sulphur Bank					
(TA1S3)	1000–1700	230	68% Metacinnabar, HgS (cub) 28% Cinnabar, HgS (hex) 10% Mercuric chloride, $HgCl_2$	90	0.137
(TA1S6)	125–250	200	77% Metacinnabar, HgS (cub) 23% Cinnabar, HgS (hex)	100	0.081
(TA1S9)	32–45	320	83% Metacinnabar, HgS (cub) 17% Cinnabar, HgS (hex)	100	0.042
Sulphur Bank[a]					
(SBW9S3)	500–2000	1580	78% Cinnabar, HgS (hex) 22% Metacinnabar, HgS (cub)	100	0.422
(SBW9S6)	75–125	22310	100% Cinnabar, HgS (hex)	100	0.107
(SBW9S9)	<45	8120	78% Cinnabar, HgS (hex) 22% Metacinnabar, HgS (cub)	100	0.110

[a] Unroasted waste rock sample

calcine from the Sulphur Bank mine shows an increase in Hg concentration from 97 ppm in the 500–2000 μm size fraction to 810 ppm in the <45 μm size fraction). This trend agrees with other studies (Nelson et al., 1977; Harsh and Doner, 1981) which showed elevated concentrations of Hg-sulfides in very fine sand and silt fractions among Hg-mine wastes in northern California and Alaska. The increase in total Hg concentration with decreasing particle size is also reflected in the residual values associated with the linear combination fits (Table 5), which become smaller as particle size decreases due to increasing signal-to-noise ratios and subsequently higher quality data. The exception to this trend is the Sulphur Bank waste rock sample (SBW9), where the maximum Hg concentration is obtained at the intermediate particle size range.

In addition to total Hg concentration, the relative proportions of Hg-sulfides (cinnabar, metacinnabar and corderoite) in the sieved fractions of calcines also increase with decreasing particle size as seen in Table 5. This trend is slight, increasing between 8–18% among the samples studied, yet in most cases the increase is greater than the operationally defined ±10% accuracy limit of EXAFS analysis, indicating that it is a significant and detectable phenomenon. The Sulphur Bank waste rock consists entirely of Hg-sulfides in all size fractions, so this trend cannot be discerned in this sample. However, the two samples from separate calcine piles at the Sulphur Bank mine both show an increase in Hg-sulfides with decreasing particle size and have very similar speciation results.

Heavy metal enrichment with decreasing particle size has been documented in marine sediments (Turekian, 1977) and contaminated floodplain sediments (Moore et al., 1989) and is typically attributed to enhanced metal sorption processes (due to both higher proportions of strongly-sorbing Fe/Mn (hydr)oxides and organic matter (Krauskopf, 1956) as well as increased reactive surface areas as particle size diminishes). However, the speciation results in Table 5 show that there is no detectable sorbed Hg present in any of the sieved fractions, indicating that enhanced sorption is not an explanation of the increases in total Hg and Hg-sulfides with decreasing particle size.

Instead, these trends may be linked to the low solubility and low hardness of cinnabar and metacinnabar. As Hg-sulfides feature K_{sp} values in the range of 10^{-36} (Schwarzenbach and Widmer, 1963) and hardness levels of 2.5–3 (Klein and Hurlbut, 1985), physical weathering processes are expected to dominate over chemical weathering processes, i.e. dissolution, and additionally should weather at more rapid rates than the harder matrix minerals such as quartz and metal oxides that comprise the bulk of the samples. Preferential mechanical weathering over chemical weathering in this manner would yield the observed enrichment in total Hg among the finer-grained size fractions. Furthermore, with decreasing particle size the increased exposure of soluble Hg minerals such as Hg-chlorides, oxides and sulfates would facilitate dissolution of these phases, resulting in the increased proportions of highly insoluble Hg-sulfides observed in the finest-grained fractions. A study of Hg speciation in stream sediments of the Almaden cinnabar mining region in Spain described a similar relationship between the proportion of Hg present as Hg-sulfides and total Hg concentration (Martin-Doimeadios et al., 2000). The results of the present study together with those previously mentioned indicate that these trends are common in cinnabar mine environments.

The Sulphur Bank waste rock sample does not exhibit the patterns of increasing total Hg concentration and proportion of Hg-sulfides with decreasing particle size as observed in the calcines. The maximum in total Hg concentration in an intermediate particle size range may instead reflect the initial size of cinnabar particles formed during Hg ore deposition in this system. Additionally, the high Hg concentrations and dominance of Hg-sulfides in waste rock may mask the presence of minor proportions of non-Hg-sulfide phases, so possible trends in Hg speciation with particle size are not detectable in waste rock. The fact that waste rock does not undergo the crushing and roasting procedures associated with calcines implies that calcining is a critical process that may be responsible for the relationships observed between particle size, total Hg concentration, and proportion of Hg-sulfides. These trends appear to extend to the colloidal size fraction as well. Column experiments using Hg calcines from the New Idria and Sulphur Bank mines show substantial release of particulate Hg in the effluents (Lowry et al., submitted for publication). EXAFS spectroscopy, CVAFS, and transmission electron microscopy (TEM) analysis of these fine-grained particles, many as small as 20 nm, indicate that essentially all of the released Hg is particle-bound and consists dominantly of Hg-sulfides (Shaw et al., in review).

3.4. Distance from source

The speciation of Hg in calcines and distributed sediments or precipitates located downstream from the calcine piles is shown in Table 6. Hg-bearing streambed sediments were sampled near the Dawson mine, and an amorphous Fe-oxyhydroxide precipitate forming downstream from an acid mine drainage seep was sampled near the Knoxville mine; both were compared with correlating calcine piles located upstream near the original mine processing facilities. Despite the different bulk compositions and locations of the samples collected at each mine, the Hg speciation of sediments/precipitates correlates very closely with that of the

Table 6
Hg speciation of calcines and distributed Hg-bearing sediments/precipitates located downstream from mine-impacted regions

Sample location	Material	Hg conc. (ppm)	EXAFS Speciation	Residual
Dawson Mine, CA				
(21DUC10)	Mine calcines	78	80% Metacinnabar, HgS (cub) 20% Cinnabar, HgS (hex)	0.146
(21DS8)	Downstream sediments	234	54% Metacinnabar, HgS (cub) 46% Cinnabar, HgS (hex)	0.098
Knoxville Mine, CA				
(MC-KN1B)	Mine calcines	277	54% Cinnabar, HgS (hex) 34% Metacinnabar, HgS (cub) 12% Mercuric chloride, $HgCl_2$	0.556
(95KN4S)	Fe-oxyhydroxide	220	42% Metacinnabar, HgS (cub) 39% Cinnabar, HgS (hex) 19% Mercuric chloride, $HgCl_2$	0.148

respective calcines. In all cases, Hg is present dominantly in the solid mineral phase, and does not appear to be present in significant proportions as Hg sorbed to particulate surfaces. These results indicate that Hg in mine tailings remains in the crystalline solid form during its release and transport from its source and that distribution does not alter speciation substantially. Any potential changes in speciation over longer distances are likely to be linked to the particle size relationship with Hg speciation discussed in the previous section. If so, one would expect further enrichment in Hg-sulfides with increasing distance from the source, where very fine-grained or colloidal Hg-bearing particles should dominate.

The identification of crystalline Hg species in the Knoxville Fe-oxyhydroxide precipitate again challenges the assumption that Hg associated with very fine-grained, high surface area precipitates is primarily present as sorbed Hg. Instead, as observed directly by Shaw et al. (submitted for publication), it is possible for Hg to exist among these precipitates as coherent submicron particles of Hg minerals.

3.5. Phase transformation of elemental Hg

Table 7 shows the Hg speciation of two Au mine tailings samples from separate ore milling sites in the Carson River basin, Nevada, where between 7000 and 7500 tons of elemental Hg(0) was lost to the environment during the use of Hg in the amalgamation and recovery of Au and Ag (Miller et al., 1998). Although identification of elemental Hg(0) in natural samples using EXAFS methods is difficult due to its lack of local structure and low-amplitude EXAFS spectrum (Fig. 2), the relatively large amplitudes visible in the EXAFS spectra of these samples, as observed with the Bessels Mill sample in Fig. 4, indicate that more structured Hg phases must be present in addition to Hg(0). Indeed, EXAFS analysis identifies significant proportions of Hg-sulfides and schuetteite in the samples. While this does not preclude the presence of Hg(0) in the sample, the identification of non-Hg(0) phases suggests a conversion of the initial Hg(0) phase to more stable forms.

Pyrolitic and sequential extractions of both samples conducted by Sladek et al. (2002) confirm that the Hg

Table 7
Hg speciation of Au mill tailings samples from the Carson River, NV mining region, where Hg was originally introduced as elemental Hg(0)

Sample Location	Material	Hg conc. (ppm)	EXAFS Speciation	Residual
Bessels Mill				
(BMCR)	Au mill tailings	1070	42% Cinnabar, HgS (hex) 39% Metacinnabar, HgS (cub) 19% Schuetteite, $Hg_3O_2SO_4$	0.057
Park & Bowie Mill				
(PB1)	Au mill tailings	217	70% Cinnabar, HgS (hex) 30% Metacinnabar, HgS (cub)	0.188

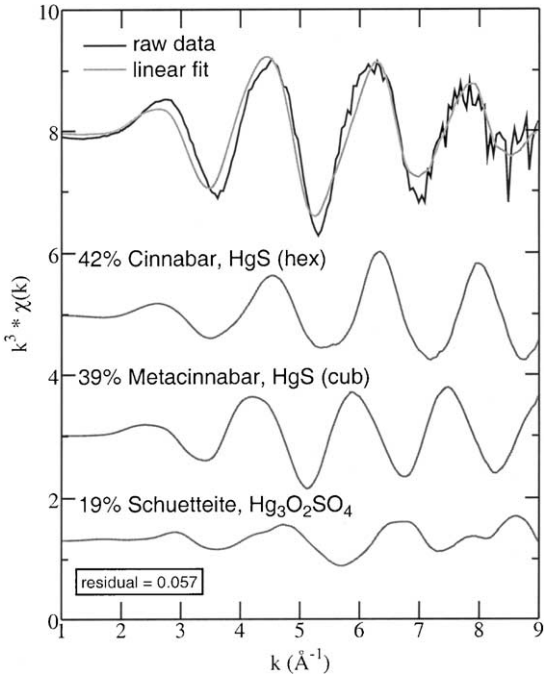

Fig. 4. Linear fitting results for the Bessels Mill, Carson River, NV sample, showing the best linear combination fit (top, gray) and the components which contribute to the linear fit.

present is less available than pure elemental Hg(0) and appears to be matrix-bound or amalgamated with other heavy metals. SEM-EDS analysis identified a combination of Hg amalgamated with Ag and/or Au, Hg associated with acanthite (Ag_2S) and other sulfides, and HgS with no detectable Ag (Sladek et al., 2002). The absence of Hg amalgams and other mixed-metal sulfides from the EXAFS model compound database does not allow their identification using linear combination fitting, although they are likely to exist in Au mine tailings and perhaps constitute the dominant Hg phase present. However, the formation of authigenic HgS particles has been observed in contaminated soils (Barnett et al., 1997) and has been proposed in the Carson River system by Lechler et al. (1997). Based on sequential extractions performed on Carson River samples, this latter study suggests that Hg dissolves out of amalgam particles and adsorbs to fine-grained sediments. Later burial in reducing high S environments fixes the Hg as HgS. The identification of Hg-sulfides and sulfates by EXAFS is consistent with this interpretation. The transformation of Hg(0) to less mobile and toxic forms over time by pathways such as those described above mitigates the environmental impact of elemental Hg contamination in former Au mining areas such as the Carson River system and the Sierra Nevada foothills.

4. Conclusions

Numerous environmental variables can influence the speciation of Hg in mine-impacted regions, subsequently affecting the potential transport, fate, and bioavailability of Hg in these systems. EXAFS spectroscopy is one of the few direct techniques for determining Hg speciation in relatively low-concentration samples such as mine wastes. The application of this method to samples spanning wide ranges of Hg concentrations, waste media, particle size, and geological background allows a more thorough analysis of the factors that may have the largest impact on Hg speciation.

The geological origin of Hg ores in the California Coast Range has a clear influence on Hg speciation, as noted previously (Kim et al., 2000) and further supported in this more extensive study of Hg mine wastes from both silica-carbonate and hot-spring depositional environments. Hot-spring deposits are more likely to host Hg-chloride phases, which tend to be much more soluble than Hg-sulfides and therefore pose significantly greater risks of releasing dissolved Hg to local surface waters. This suggestion is consistent with the elevated fluxes of atmospheric Hg emission measured by Gustin et al. (2002a) in hydrothermal regions and indicates that remediation efforts should be focused on these sites.

Anthropogenic processes such as ore roasting also have observable effects on Hg speciation, primarily through the conversion of cinnabar to metacinnabar. The impact of this phase transformation on Hg release may not be significant, however, as the solubilities of both phases are equally low. However, another study by Gustin et al. (2002b), which reports higher light-enhanced Hg emissions in samples containing metacinnabar compared to those containing exclusively cinnabar, indicates that the specific Hg-sulfide phase influences the atmospheric evasion of Hg and may also affect aqueous Hg release. The increased exposure and potential mobility of calcines as a result of the crushing and roasting they undergo justify their highest priority classification for remediation at Hg-contaminated sites.

The introduction of elemental Hg(0) to Au mine regions is another anthropogenic process with potentially significant environmental consequences, as EXAFS analysis suggests that the initial Hg(0) has converted over time to more stable phases such as Hg-sulfides and schuetteite, a finding that is consistent with sequential extraction and pyrolitic extraction studies. The low solubilities of these species relative to Hg(0) further indicate that the Hg present in Au mine tailings may pose less of a threat than previously thought.

Particle size is a variable that affects both the bulk Hg concentration and Hg speciation in a sample. Again, this is a significant concern in calcine piles, where the trends of increasing total Hg and proportion of Hg-sulfides with decreasing particle size are apparent. The

accelerated weathering of these materials through the calcining process and their subsequent exposure to natural weathering processes have likely produced the observed trends, as size-dependent studies of unroasted waste rock do not yield similar patterns. The elevated Hg concentrations in the finest-grained fractions of Hg calcines are of significant concern, as the high transport potential of colloidal particles can lead to greater dispersion and contamination of Hg over long distances in aquatic systems.

Mercury speciation over distances is relatively unaffected by distribution from the source based on EXAFS analysis of calcines and related downstream sediments and precipitates. This result is likely due to the high proportion of stable Hg-sulfides present in the fine-grained fraction of mobile suspended particles. However, the potential for Hg release from these phases over long time spans, combined with their extensive dispersal from mine-impacted regions, suggests that the transport of colloidal Hg-bearing particulates is an important process controlling Hg contamination in larger environmental systems.

Identification of the primary factors influencing Hg speciation in mine wastes is critical in providing a more detailed and accurate assessment of a contaminated site beyond just total Hg concentration. EXAFS spectroscopy and additional characterization techniques, such as TEM and sequential chemical extractions, are needed to provide this type of assessment and to help prioritize and direct remediation efforts among the multiple mine-impacted regions in the California Coast Range.

Acknowledgements

This study was supported by the US Environmental Protection Agency-Science To Achieve Results program (US EPA-STAR program grant EPA-R827634-01-1) and the U.S. Geological Survey, Geologic Division. We wish to acknowledge the staff of the Stanford Synchrotron Radiation Laboratory, particularly John Bargar and Joe Rogers for their assistance during EXAFS data collection on Beamline 11-2. SSRL is supported by the US Department of Energy (BES and BER) and the National Institutes of Health. Mae Gustin and Chris Sladek of the University of Nevada-Reno provided several samples from Nevada and the McLaughlin Hg district. We also thank two anonymous reviewers whose input helped improve the paper.

References

Barnes, I., Hinkle, M.E., Rapp, J.B., Heropoulos, C., Vaughn, W.W., 1973a. Chemical Composition of Naturally Occurring Fluids in Relation to Mercury Deposits in Part of North Central California. US Geological Survey.

Barnes, I., O'Neil, J.R., Rapp, J.B., White, D.E., 1973b. Silica-carbonate alteration of serpentinite: wall rock alteration in mercury deposits of the California Coast Ranges. Econ. Geol. 68, 388–398.

Barnett, M.O., Harris, L.A., Turner, R.R., Stevenson, R.J., Henson, T.J., Melton, R.C., Hoffman, D.P., 1997. Formation of mercuric sulfide in soil. Environ. Sci. Technol. 31, 3037–3043.

Brown Jr., G.E., Parks, G.A., 1989. Synchrotron-based X-ray absorption studies of cation environments in earth materials. Rev. Geophys. 27, 519–533.

Carlson, E.E., 1967. The growth of HgS and $Hg_3S_2Cl_2$ single crystals by a vapor phase method. J. Cryst. Growth 1, 271–277.

Churchill, R., 1999. Insights into California mercury production and mercury availability for the gold mining industry from the historical record. Geol. Soc. Am. Abs. 31, 45.

Cotter-Howells, J.D., Champness, P.E., Charnock, J.M., Pattrick, R.A.D., 1994. Identification of pyromorphite in mine-waste contaminated soils by ATEM and EXAFS. Eur. J. Soil. Sci. 45, 393–402.

Dickson, F.W., Tunell, G., 1959. The stability relations of cinnabar and metacinnabar. Am. Mineral. 44, 471–487.

Dickson, F.W., Tunell, G., 1968. Mercury and antimony deposits associated with active hot springs in the western United States. In: Ridge, J.D. (Ed.), Ore Deposits of the United States, 1933-1967. The American Institute of Mining, Metallurgical, and Petroleum Engineers, Inc, New York, NY, pp. 1673–1701.

Drummond, S.E., Ohmoto, H., 1985. Chemical evolution and mineral deposition in boiling hydrothermal systems. Econ. Geol. 80, 126–147.

EPA, 2001. Method 1631, Revision C: Mercury in Water by Oxidation, Purge and Trap, and Cold Vapor Atomic Fluorescence Spectrometry. Environmental Protection Agency, EPA-821-R-01-24, Washington, DC.

Foord, E.E., Berendsen, P., 1974. Corderoite, first natural occurrence of a-$Hg_3S_2Cl_2$, from the Cordero mercury deposit, Humboldt County, Nevada. Am. Mineral. 59, 652–655.

Foster, A.L., Brown Jr., G.E., Tingle, T., Parks, G.A., 1998. Quantitative arsenic speciation in mine tailings using X-ray absorption spectroscopy. Am. Mineral. 83, 553–568.

Ganguli, P.M., Mason, R.P., Abu-Saba, K.E., Anderson, R.S., Flegal, A.R., 2000. Mercury speciation in drainage from the New Idria mercury mine, California. Environ. Sci. Technol. 34, 4773–4779.

George, G.N., Pickering, I.J., 1995. EXAFSPAK, a Suite of Computer Programs for the Analysis of X-ray Absorption Spectra. Stanford Synchrotron Radiation Laboratory, Stanford, CA.

Gustin, M.S., Coolbaugh, M., Engle, M., Fitzgerald, B., Keislar, R., Lindberg, S., Nacht, D., Quashnick, J., Rytuba, J.J., Sladek, C., Zhang, H., Zehner, R.E., 2002a. Atmospheric mercury emissions from mine wastes and surrounding geologically enriched terrains. Environ. Geol. 43, 339–351.

Gustin, M.S., Biester, H., Kim, C.S., 2002b. Investigation of the light-enhanced emission of mercury from naturally enriched substrates. Atmos. Environ. 36, 3241–3254.

Gustin, M.S., Lindberg, S.E., Austin, K., Coolbaugh, M., Vette, A., Zhang, H., 2000. Assessing the contribution of

natural sources to regional atmospheric mercury budgets. Sci. Total Environ. 259, 61–71.

Harsh, J.B., Doner, H.E., 1981. Characterization of mercury in a riverwash soil. J. Environ. Qual. 10, 333–337.

Henley, R.W., 1985. The geothermal framework for epithermal deposits. In: Berger, B.R., Bethke, P.M. (Eds.), Geology and Geochemistry of Epithermal Systems. Society of Economic Geologists, New York, NY, pp. 1–24.

Isaure, M.P., Laboudigue, A., Manceau, A., Sarret, G., Tiffreau, C., Trocellier, P., Lamble, G., Hazemann, J.L., Chateigner, D., 2002. Quantitative Zn speciation in a contaminated dredged sediment by M-PIXE, M-SXRF, EXAFS spectroscopy and principal component analysis. Geochim. Cosmochim. Acta 66, 1549–1567.

Juillot, F., Morin, G., Ildefonse, P., Trainor, T.P., Benedetti, M., Galoisy, L., Calas, G., Brown Jr., G.E., 2003. Occurrence of Zn/Al hydrotalcite in smelter-impacted soils from Northern France: evidence from EXAFS spectroscopy and chemical extractions. Am. Mineral. 88, 509–526.

Kim, C.S., Bloom, N.S., Rytuba, J.J., G.E. Brown, J. Mercury speciation by extended X-ray absorption fine structure (EXAFS) spectroscopy and sequential chemical extractions: a comparison of speciation methods. Environ. Sci. Technol. (in press).

Kim, C.S., Brown Jr., G.E., Rytuba, J.J., 2000. Characterization and speciation of mercury-bearing mine wastes using X-ray absorption spectroscopy (XAS). Sci. Total Environ. 261, 157–168.

Klein, C., Hurlbut Jr., C.S., 1985. Manual of Mineralogy. John Wiley & Sons, Inc, New York, NY.

Krauskopf, K.B., 1956. Factors controlling the concentrations of thirteen rare metals in sea-water. Geochim. Cosmochim. Acta 10, 1–26.

Kullerud, G., 1965. The mercury-sulfur system. Carnegie I 64, 194–195.

Lechler, P.J., Miller, J.R., Hsu, L.C., Desilets, M.O., 1997. Mercury mobility at the Carson River Superfund Site, west-central Nevada, USA: interpretation of mercury speciation data in mill tailings, soils, and sediments. J. Geochem. Explor. 58, 259–267.

Lowry, G.V., Shaw, S., Kim, C.S., Rytuba, J.J., Brown, G.E., Jr. Particle-facilitated mercury transport from New Idria and Sulphur Bank mercury mine tailings: 1. Column experiments and macroscopic analysis. Environ. Sci. Technol. (in review).

Manceau, A., Boisset, M.C., Sarret, G., Hazemann, J.L., Mench, M., Cambier, P., Prost, R., 1996. Direct determination of lead speciation in contaminated soils by EXAFS spectroscopy. Environ. Sci. Technol. 30, 1540–1552.

Manceau, A., Lanson, B., Schlegel, M.L., Harge, J.C., Musso, M., EybertBerard, L., Hazemann, J.L., Chateigner, D., Lamble, G.M., 2000. Quantitative Zn speciation in smelter-contaminated soils by EXAFS spectroscopy. Am. J. Sci. 300, 289–343.

Martin-Doimeadios, R.C.R., Wasserman, J.C., Bermejo, L.F.G., Amouroux, D., Nevado, J.J.B., Donard, O.F.X., 2000. Chemical availability of mercury in stream sediments from the Almaden area, Spain. J. Environ. Monitor 2, 360–366.

Miller, J.R., Lechler, P.J., Desilets, M., 1998. The role of geomorphic processes in the transport and fate of mercury in the Carson River basin, west-central Nevada. Environ. Geol. 33, 249–262.

Moore, J.N., Brook, E.J., Johns, C., 1989. Grain-size partitioning of metals in contaminated, coarse-grained river floodplain sediment: Clark Fork River, Montana, United States. Environ. Geol. Water S 14, 107–115.

Morin, G., Ostergren, J.D., Juillot, F., Ildefonse, P., Calas, G., Brown Jr., G.E., 1999. XAFS determination of the chemical form of lead in smelter-contaminated soils and mine tailings: importance of adsorption processes. Am. Mineral. 84, 420–434.

Nelson, H., Larsen, B.R., Jenne, E.A., Sorg, D.H., 1977. Mercury dispersal from lode sources in Kuskokwim River drainage, Alaska. Science 198, 820–824.

O'Day, P.A., Carroll, S.A., Waychunas, G.A., 1998. Rock-water interactions controlling zinc, cadmium, and lead concentrations in surface waters and sediments, US Tri-State Mining District. 1. Molecular identification using X-ray absorption spectroscopy. Environ. Sci. Technol. 32, 943–955.

Ostergren, J.D., Brown Jr., G.E., Parks, G.A., Tingle, T.N., 1999. Quantitative speciation of lead in selected mine tailings from Leadville, CO. Environ. Sci. Technol. 33, 1627–1636.

Paquette, K., Helz, G., 1995. Solubility of cinnabar (red HgS) and implications for mercury speciation in sulfidic waters. Water, Air, Soil Pollut. 80, 1053–1056.

Parks, G.A., Nordstrom, D.K., 1979. Estimated free energies of formation, water solubilities, and stability fields for schuetteite ($Hg_3O_2SO_4$) and corderoite ($Hg_3S_2Cl_2$) at 298 K. ACS Symp. Ser. 93, 339–352.

Peabody, C.E., Einaudi, M.T., 1992. Origin of petroleum and mercury in the Culver-Baer Cinnabar deposit, Mayacmas District, California. Econ. Geol. 87, 1078–1103.

Roth, D.A., Taylor, H.E., Domagalski, J., Dileanis, P., Peart, D.B., Antweiler, R.C., Alpers, C.N., 2001. Distribution of inorganic mercury in Sacramento River water and suspended colloidal sediment material. Arch. Environ. Contam. Toxicol. 40, 161–172.

Rytuba, J.J., 1996. Cenozoic metallogeny of California. In: Geology and Ore Deposits of the American Cordillera Symp. Proc., Reno, NV, 803–822.

Rytuba, J.J., 2000. Mercury mine drainage and processes that control its environmental impact. Sci. Total Environ. 260, 57–71.

Schwarzenbach, G., Widmer, M., 1963. Die Loslichkeit von Metallsulfiden I. Schwarzes Quecksilbersulfid. Helv. Chim. Acta 46, 2613–2628.

Shaw, S., Lowry, G.V., Kim, C.S., Rytuba, J.J., Brown, G.E., Jr. Particle-facilitated mercury transport from New Idria and Sulphur Bank mercury mine tailings: 2. Microscopic, spectroscopic, and chemical analyses of colloidal material. Environ. Sci. Technol. (in review).

Sherlock, R.L., Logan, M.A.V., 1995. Silica-carbonate alteration of serpentinite: implications for the association of mercury and gold mineralization in Northern California. Explor. Min. Geol. 4, 395–409.

Sherlock, R.L., Tosdal, R.M., Lehrman, N.J., Graney, J.R., Losh, S., Jowett, E.C., Kesler, S.E., 1995. Origin of the McLaughlin Mine sheeted vein complex: metal zoning, fluid inclusion, and isotopic evidence. Econ. Geol. 90, 2156–2181.

Sladek, C., Gustin, M.S., Biester, H., Kim, C.S., 2002. Assessment of three methods for determining mercury speciation in mine waste. Geochem. Explor. Environ. Anal. 2, 369–375.

Tauson, V.L., Akimov, V.V., 1997. Introduction to the theory of forced equilibria: General principles, basic concepts, and definitions. Geochim. Cosmochim. Acta 61, 4935–4943.

Turekian, K.K., 1977. Fate of metals in oceans. Geochim. Cosmochim. Acta 41, 1139–1144.

Waychunas, G.A., Brown Jr., G.E., 1994. Fluorescence yield XANES and EXAFS experiments: application to highly dilute and surface samples. Adv. X-Ray Anal. 37, 607–617.

White, D.E., Roberson, C.E., 1962. Sulphur Bank, California: a major hot-spring quicksilver deposit. In: Engel, A.E.J., James, H.L., Leonard, B.F. (Eds.), Petrologic Studies: A Volume in Honor of A.F. Buddington. The Geological Society of America, pp. 397–428.